Investigation of the inhomogeneous barrier height of an $Au/Bi_4Ti_3O_{12}/n$-Si structure through Gaussian distribution of barrier height*

M. Gökçen† and M. Yıldırım

Department of Physics, Faculty of Arts and Sciences, Düzce University, Düzce, Turkey

(Received 19 June 2012; revised manuscript received 24 July 2012)

A $Au/Bi_4Ti_3O_{12}/n$-Si structure is fabricated in order to investigate its current–voltage (I–V) characteristics in a temperature range of 300 K–400 K. Obtained I–V data are evaluated by the thermionic emission (TE) theory. Zero-bias barrier height (Φ_{B0}) and ideality factor (n) calculated from I–V characteristics, are found to be temperature-dependent such that Φ_{B0} increases with temperature increasing, whereas n decreases. The obtained temperature dependence of Φ_{B0} and linearity in Φ_{B0} versus the n plot, together with a lower barrier height and Richardson constant values obtained from the Richardson plot, indicate that the barrier height of the structure is inhomogeneous in nature. Therefore, I–V characteristics are explained on the basis of Gaussian distribution of barrier height.

Keywords: $Bi_4Ti_3O_{12}$, I–V characterization, temperature dependence, Gaussian distribution

PACS: 85.30.Hi, 85.30.Kk, 84.37.+q, 73.40.–c **DOI:** 10.1088/1674-1056/21/12/128502

1. Introduction

Ferroelectrics have proven to be important materials in thin film applications due to their properties of spontaneous polarization which can be reversed through reversing the applied external electric field. Bismuth titanate ($Bi_4Ti_3O_{12}$) ferroelectric is a typically ferroelectric material of perovskite oxide structure. Thin films of $Bi_4Ti_3O_{12}$ are ideal materials for non-volatile random access memories (NVRAMs), optical memories, piezoelectric and electro–optic devices due to their favourable properties such as high dielectric constants, high polarization charge densities, high fatigue endurances, and high transmittances.[1−7]

Interfaces between various layers of heterostructures are important parts of electronic and optoelectronic devices. One of the most interesting features of interfaces is their Schottky barrier height (SBH), which is a measure of the mismatch of the energy levels for the majority carriers across the interface. The performance of a heterostructure device is strongly dependent on the homogeneity of interface in the structure. Poor interfaces between the insulator film and Si in Schottky barrier diodes (SBDs) and metal–insulator-semiconductor (MIS) based devices lead to high leakage currents and high defect trapped charges. When a ferroelectric thin film is utilized in an SBD and MIS-based device, the leakage current under a direct current electric field has a smaller value. Therefore, using a high-dielectric material such as $Bi_4Ti_3O_{12}$ at the metal/semiconductor (M/S) interface improves the performance and reliability of the device.

Generally, the analysis of the forward bias current–voltage (I–V) characteristics of an SBD and/or MIS-based structure only at room temperature does not give detailed information about the conduction mechanism and barrier formation at the M/S interface. However, temperature-dependent I–V measurements allow one to understand different aspects of the conduction process in the device.[8−13] The possible mechanisms of charge carrier transport through the barrier may be thermionic emission (TE), thermionic field emission (TFE), recombination–generation (RG), interface recombination tunneling, minority carrier injection, and tunneling via interface states or dislocations.[14,15] The analyses of the I–V characteristics of SBD- and MIS-based structures, based on the thermionic emission theory, usually reveal an anomalous decrease in the barrier height (BH) and an increase in the ideality factor (n) with temperature decreasing, which leads to non-linearity in the

*Project supported by the Düzce University Scientific Research Project (Grant Nos. 2010.05.02.056 and 2012.05.02.110).

†Corresponding author. E-mail: muharremgokcen@duzce.edu.tr

© 2012 Chinese Physical Society and IOP Publishing Ltd

activation energy obtained from the $\ln(I_0/T^2)$ versus $1/T$ plot.[12,16,17] This anomalous behaviour can be understood only on the basis of the spatial distribution of BH at the contact interface. The distribution of BH is described mainly by the Gaussian distribution (GD) function. The GD is believed to be the only possible model to explain the observed temperature dependence of barrier parameters.[16–18] Over the last few years, the GD approach to inhomogeneous barrier height has been used in various studies.[19–22] The origin of reducing BH and increasing n with temperature decreasing has been successfully explained on the basis of a TE theory with a GD of BH in some studies.[9,14,21,22]

In the present study, we fabricate a $Au/Bi_4Ti_3O_{12}$/n-Si structure and study the temperature-dependent electrical transport behaviour in order to evaluate the values of BH and n. The temperature dependencies of Φ_{B0} and n in $Au/Bi_4Ti_3O_{12}$/n-Si structures are explained on the basis of the existence of GD of the BH due to BH inhomogeneity at the M/S interface.

2. Experiment

The studied $Au/Bi_4Ti_3O_{12}$/n-Si structure was fabricated using a n-type (P-doped) single crystal silicon wafer with ⟨110⟩ surface orientation, 280-μm thick, 3-mm diameter, and 4.45-Ω·cm resistivity. In the first step of cleaning, the wafer was ultrasonically cleaned by acetone, propanol, and de-ionized water, each for 10 min sequentially. Following the first step, the piranha solution ($3H_2SO_4$:$1H_2O_2$) was prepared for cleaning the organic residues. Then, the wafer was immersed into the solution for 15 min. In the last step, the wafer was dipped into the solution of 20% HF to get rid of the oxide layer formed in the previous step. After each cleaning step, the wafer was rinsed thoroughly in de-ionized water of 18 MΩ-cm resistivity. Immediately after surface cleaning, high-purity Au metal (99.999%) with a thickness of 2500 Å (1 Å=0.1 nm) was thermally evaporated from the tungsten filament onto the whole back surface of the wafer in a liquid nitrogen-trapped vacuum system with a pressure of 1.33×10^{-4} Pa. In order to achieve a good Ohmic contact, the evaporated Au was annealed at 700 °C for 20 min. The front side of the wafer was cleaned with 20% HF solution to remove the thin oxide layer which had been formed during annealing. Then, the wafer was cut into a few pieces. In order to form $Au/Bi_4Ti_3O_{12}$/n-Si structure, the $Bi_4Ti_3O_{12}$ film was prepared onto the front side of the Si wafer by the use of magnetron sputtering with the hot compacting of $Bi_4Ti_3O_{12}$ powder of a stochiometric composition serving as the target material. A mixture of Ar and O_2 was used as a working medium and the substrate was kept at 700 °C. The thickness values of the deposited BTO thin films were found to average around 250 Å measured by the Veeco Dektak 6M thickness profilometer. After the $Bi_4Ti_3O_{12}$ film was deposited onto the Si wafer, circular dots 2 mm in diameter and with 2500-Å thick Au rectifying contacts were deposited onto the film surface of the wafer through a metal shadow mask by a thermal evaporator vacuum system with a pressure of 1.33×10^{-4} Pa. The thickness of the metal layer and deposition rates were both monitored with the help of a digital quartz crystal thickness monitor. The deposition rates were about 1 Å/s–3 Å/s.

The current–voltage (I–V) measurements of the $Au/Bi_4Ti_3O_{12}$/n-Si structure were performed using a Keithley 2400 source-meter at various temperatures ranging from 300 K to 400 K in steps of 10 K.

3. Results and discussion

In general, current passing through the $Au/Bi_4Ti_3O_{12}$/n-Si structure in the forward bias region can be explained on the basis of the TE theory where $V \geq 3kT/q$. According to the TE theory, the relationship between I and V is given by[10,21]

$$I = I_0 \left[\exp\left(\frac{qV}{nkT}\right) - 1\right]. \tag{1}$$

Here, n, T, k, q, and I are the ideality factor, absolute temperature in Kelvin, Boltzmann constant, electronic charge, and reverse saturation current, respectively. The reverse saturation current is defined as[10,21]

$$I_0 = AA^*T^2 \exp\left(-\frac{q\Phi_{B0}}{kT}\right), \tag{2}$$

where A^* and A are the effective Richardson constant (120 A/cm^2·K^2 for n-Si) and area of rectifying contact, respectively.

Obtained I–V data are represented in a semi-logarithmic I–V plot which is given in Fig. 1, and the data were evaluated by the TE theory. As shown in Fig. 1, temperature-dependent dispersion behaviour in the reverse bias region is obvious compared with that in the forward bias region. Furthermore, the

leakage current increases as the temperature increases. However, the leakage current reaches a saturation value at a lower reverse bias voltage values. This may be attributed to the space–charge region expanding as the temperature increases. Also, as explained in various studies,[10−12,14,23,24] forward bias I–V plots bend due to the effect of R_s. As to the evaluation of TE theory, when equation (1) is taken into consideration, the values of n and Φ_{B0} are extracted from the slope and intersection point of $\ln(I)$–V plots using the following equations:[10,19,23−25]

$$n = \frac{q}{kT}\left(\frac{\mathrm{d}V}{\mathrm{d}(\ln I)}\right), \tag{3a}$$

$$\Phi_{B0} = \frac{kT}{q}\ln\left[\frac{AA^*T^2}{I_0}\right]. \tag{3b}$$

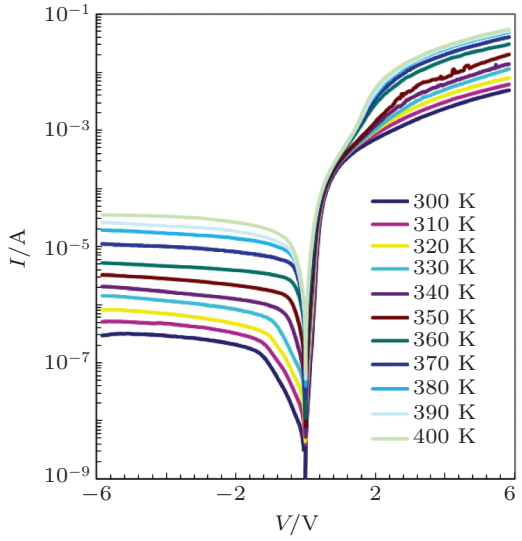


Fig. 1. (colour online) Semi-logarithmic I–V plots of the $Au/Bi_4Ti_3O_{12}$/n-Si structure at various temperatures.

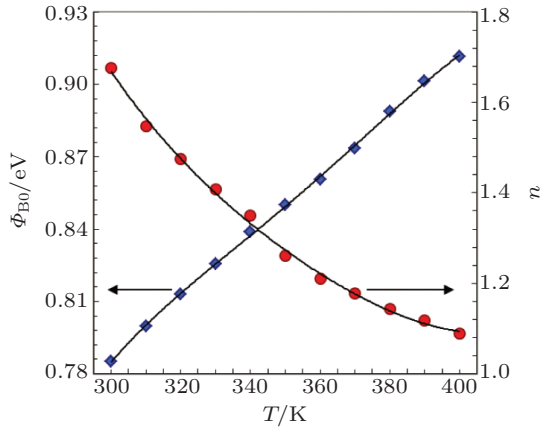


Fig. 2. (colour online) Φ_{B0} and n versus T plots of $Au/Bi_4Ti_3O_{12}$/n-Si structure.

The calculated values of n and Φ_{B0} are given in Table 1, and they are also given in Fig. 2 each as a function of temperature. As can be seen in Table 1 and Fig. 2, the values of n and Φ_{B0} are both temperature-dependent such that n decreases and Φ_{B0} increases with temperature increasing. According to the TE theory, the value of n is expected to be close to unity. However, experimental results show that the calculated values of n are greater than unity especially at lower temperatures. This case can be attributed to the existence of an insulator layer at the M/S interface, the particular distribution of N_{ss} at the semiconductor band gap and the image force lowering of the barrier. There are various methods of determining the values of N_{ss} for an SBD- or MIS-like structure. Among them, the one proposed by Chard and Rhoderick[26] can easily be applied using the forward bias I–V data. The values of N_{ss} of the structure are calculated using this method and given in Table 1. As can be seen, the values of N_{ss} decrease as temperature increases. Such behaviour of N_{ss} is indeed consistent with the behaviour of n with temperature increasing. On the other hand, the obtained temperature dependence of Φ_{B0} indicates a positive temperature coefficient; this can be attributed to BH inhomogeneity. Temperature dependence of BH can be expressed as[1,11,21]

$$\Phi_B(T) = \Phi_B(T=0) + \alpha T, \tag{4}$$

where α is the temperature coefficient of BH and it is expected to take a negative value according to the temperature coefficient of the Si band gap. However, there is an obvious disagreement between the temperature dependence of Φ_{B0} and the temperature coefficient of the Si band gap. This discrepancy which stems from the inhomogeneity of BH, can be overcome by eliminating the image force lowering through using a flat-band barrier height (Φ_{Bf}) approach. In this approach, the semiconductor bands are flat, which eliminate the effect of image force lowering that would affect the I–V characteristics, and remove the influence of BH inhomogeneity.[12,17] Φ_{Bf} can be calculated by using experimental values of n and Φ_{B0} in the following equation:[12]

$$\Phi_{Bf} = n\Phi_{B0} - (n-1)\frac{kT}{q}\ln\left(\frac{N_C}{N_D}\right), \tag{5}$$

where N_C is the effective density of states in the Si conduction band and N_D is the donor carrier doping density of n-Si. The obtained Φ_{Bf} values, together with Φ_{B0}, are given in Table 1, and also the temperature dependencies of Φ_{Bf} and Φ_{B0} are given in Fig. 3.

As shown in Fig. 3, Φ_{B0}–T plot gives a single-linearity with $\alpha = 13\times10^{-4}$ eV/K whereas the Φ_{Bf}–T plot represents double-linearity with $\alpha_1 = -46 \times 10^{-4}$ eV/K and $\alpha_2 = -12 \times 10^{-4}$ eV/K for lower and higher temperatures, respectively. The values of α_1 and α_2 are found to be negative and are consistent with the negative temperature coefficient of the Si band gap ($\alpha_{Si} = -4.73 \times 10^{-4}$ eV/K).

Table 1. Electrical parameters of the $Au/Bi_4Ti_3O_{12}$/n-Si structure obtained from I–V characteristics at various temperatures.

T/K	I_0/A	n	Φ_{B0}/eV	Φ_{Bf}/eV	N_{ss}/eV^{-1}·cm^{-2}
300	5.60^{-9}	1.68	0.785	1.332	2.96^{13}
310	9.28^{-9}	1.55	0.800	1.251	2.39^{13}
320	1.56^{-8}	1.47	0.813	1.211	2.07^{13}
330	2.60^{-8}	1.41	0.826	1.174	1.77^{13}
340	4.14^{-8}	1.35	0.839	1.141	1.51^{13}
350	6.83^{-8}	1.26	0.850	1.079	1.12^{13}
360	1.13^{-7}	1.21	0.860	1.047	8.94^{12}
370	1.68^{-7}	1.18	0.873	1.034	7.50^{12}
380	2.27^{-7}	1.14	0.889	1.020	5.97^{12}
390	3.32^{-7}	1.12	0.901	1.011	4.86^{12}
400	5.04^{-7}	1.09	0.912	0.996	3.62^{12}

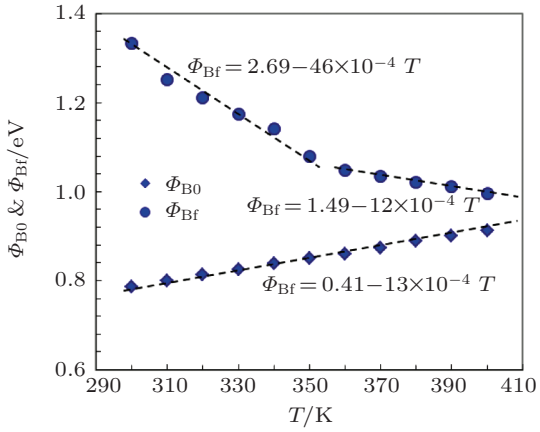


Fig. 3. (colour online) Plots of Φ_{B0} and Φ_{Bf} versus T of the $Au/Bi_4Ti_3O_{12}$/n-Si structure.

Evaluation of BH can also be made through the Richardson plot ($\ln(I/T^2)$ versus q/kT) of I_0 by arranging Eq. (2) in the following form:

$$\ln\left(\frac{I_0}{T^2}\right) = \ln(AA^*) - \frac{q}{kT}\Phi_{B0}. \tag{6}$$

The Richardson plot of the structure is given in Fig. 4. The line equation of this plot is also given in Fig. 4. The values of A^* and Φ_{B0} are obtained from the interception point and slope of this plot are 5.26×10^5 A·cm^{-2}·K^{-2} and 0.409 eV, respectively. The obtained value of A^* is much lower than its theoretical value (120 A·cm^{-2}·K^{-2}), also Φ_{B0} is found to be less than the experimental value. This implies inhomogeneous BH and potential fluctuations at the interface lead to the results of lower and higher patches of the barrier.[9,12,21]

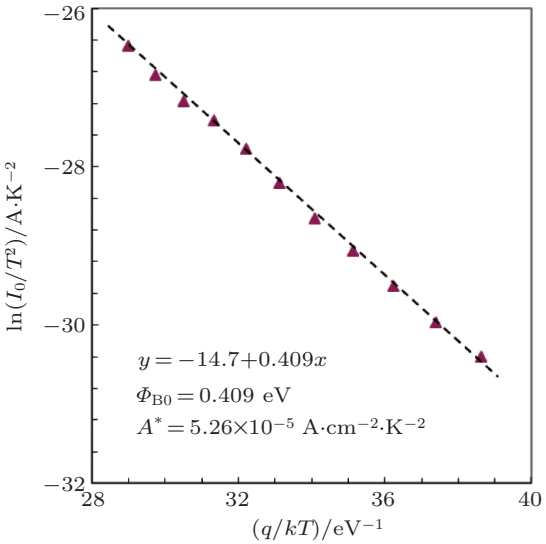


Fig. 4. The Richardson plot of the $Au/Bi_4Ti_3O_{12}$/n-Si structure.

Furthermore, Tung[16] introduced an approach in which a linear correlation between Φ_{B0} and n is taken into consideration. Proceeding with Tung's study, Schmitsdorf *et al.*[27] reached the same conclusion. Also, the studies in the last decade showed that the Φ_{B0}–n plot can have more than one linear region.[10,11,14,21] Figure 5 presents Φ_{B0} as a function

of n. As shown in the figure, the Φ_{B0}–n plot depicts two linear regions, for which line equations are given in the figure. As explained in Refs. [13], [16], [17], and [22], BH is a function of atomic structure and inhomogeneity at metal–semiconductor interface, and it is affected by various factors such as interface state, defect, etc. The behaviour of the Φ_{B0}–n plot suggests that Φ_{B0} is inversely proportional to n so that Φ_{B0} is less sensitive to change in n where $n > 1.2$ holds. This can be attributed to the lateral inhomogeneity of BH under the effect of temperature. Such behaviour together with the changes in Φ_{B0} and n with temperature shown in Fig. 2, and the inconsistent values obtained from the Richardson plot shown in Fig. 4, have been explained on the basis of the TE theory with a GD of BH by many researchers.[9–12,14,18,21,28]

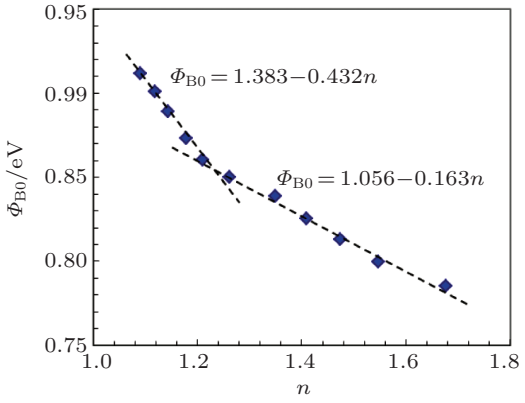


Fig. 5. (colour online) Φ_{B0}–n plot of $Au/Bi_4Ti_3O_{12}/n$-Si structure.

As offered by Werner and Güttler,[18] in the case of barrier inhomogeneity which can be explained by GD of BH, the current expression of the structure can be written as

$$I = \int_{-\infty}^{\infty} I(\Phi_B, V) P(\Phi_B) \mathrm{d}\Phi, \tag{7}$$

where $I(\Phi_B, V)$ is the current as a function of BH and applied bias voltage and $P(\Phi_B)$ is the normalization distribution function which reveals the probability of accuracy for BH, and it is given by

$$P(\Phi_B) = \frac{1}{\sigma_s\sqrt{2\pi}} \exp\left[-\frac{(\Phi_B - \overline{\Phi}_B)^2}{2\sigma_s^2}\right], \tag{8}$$

with σ_s being the standard deviation of BH. Solving Eq. (7) yields the following current expression similar to Eq. (1):

$$I = AA^*T^2 \exp\left(-\frac{q\Phi_{ap}}{kT}\right)\left[\exp\left(\frac{qV}{n_{ap}kT}\right) - 1\right], \tag{9}$$

where

$$I_0 = AA^*T^2 \exp\left(-\frac{q\Phi_{ap}}{kT}\right), \tag{10}$$

with Φ_{ap} and n_{ap} being the apparent barrier height and apparent ideality factor, respectively, and given as

$$\Phi_{ap} = \overline{\Phi}_{B0} - \frac{q}{2kT}\sigma_s^2, \tag{11}$$

$$\left(n_{ap}^{-1} - 1\right) = \rho_2 - \frac{q}{2kT}\rho_3. \tag{12}$$

Here, ρ_2 and ρ_3 are the voltage coefficients which quantify the deformation of BH distribution due to applied bias voltage, so that $\overline{\Phi}_B = \overline{\Phi}_{B0} + \rho_2 V$ and $\sigma_s = \sigma_{so} + \rho_3 V$. As can be deduced by Eq. (9), the values of Φ_{B0} and n which are given in Table 1 actually represent the values of Φ_{ap} and n_{ap}. Hence, using these values, Φ_{ap} –$q/2kT$ and n_{ap}–$q/2kT$ plots are plotted in Fig. 6. It is clear that interception point and slope of Φ_{ap}–$q/2kT$ plot reveal $\bar{\Phi}_{B0}$ and σ_s whereas those of n_{ap}–$q/2kT$ plot reveal ρ_2 and ρ_3.

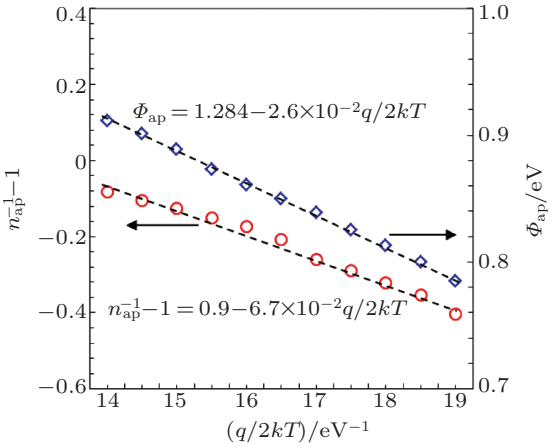


Fig. 6. (colour online) n_{ap}^{-1}–1 and Φ_{ap} versus T plots of the $Au/Bi_4Ti_3O_{12}/n$-Si structure.

Considering BH inhomogeneity and using Eqs. (10) and (11), the Richardson plot can be modified with the following equation:

$$\ln\left(\frac{I_0}{T^2}\right) - \frac{1}{2}\left(\frac{q\sigma_s}{kT}\right)^2 = \ln(AA^*) - \frac{q}{kT}\overline{\Phi}_{B0}. \tag{13}$$

A modified Richardson plot ($\ln(I/T^2)$–$1/2(q\sigma_s/kT)^2$ versus q/kT) is obtained using Eq. (13) as shown in Fig. 7. A^* and $\bar{\Phi}_{B0}$ are obtained using the interception point and slope of this plot, respectively. As shown in Fig. 7, values of A^* and $\bar{\Phi}_{B0}$ are calculated to be 136 $A\cdot cm^{-2}\cdot K^{-2}$ and 1.286 eV, respectively. The value of A^* obtained from the modified Richardson plot is close to the theoretical value of A^* for n-Si. Moreover, the values of $\bar{\Phi}_{B0}$ obtained

from Figs. 6 and 7 are in very good agreement with each other.

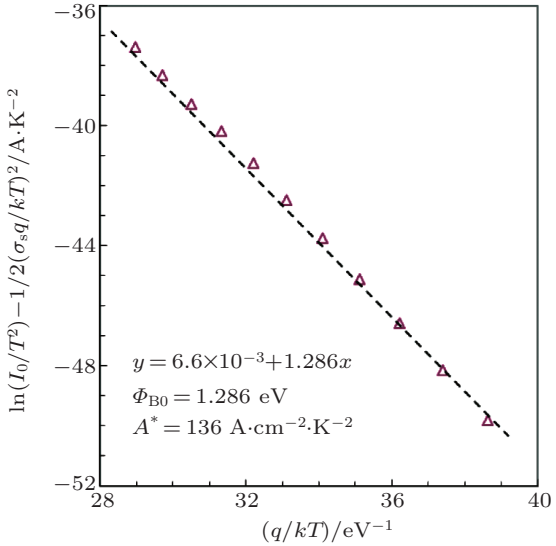


Fig. 7. (colour online) Modified Richardson plot of the $Au/Bi_4Ti_3O_{12}/n$-Si structure.

4. Conclusions

The I–V characteristics of a $Au/Bi_4Ti_3O_{12}/n$-Si structure were investigated in a temperature range of 300 K–400 K. Barrier height (BH) and ideality factor (n) calculated from I–V characteristics based on TE theory, were found to be temperature-dependent so that BH increases and n decreases with temperature increasing. The obtained temperature dependence of BH and linearity in BH versus n plot, together with lower BH and A^* values obtained from the Richardson plot indicate that BH is inhomogeneous in nature. Inhomogeneous behaviour of BH is approached with the Gaussian distribution of BH, thus a modified Richardson plot yields BH and A^* values that are close to theoretical ones.

References

[1] Altındal Ş, Parlaktürk F, Tataroğlu A, Parlak M, Sarmasov S N and Agasiev A A 2008 *Vacuum* **82** 1246

[2] Yang C H, Wang S D and Yang D M 2009 *J. Alloys Compd.* **467** 434

[3] Han J P and Ma T P 1998 *Appl. Phys. Lett.* **72** 1185

[4] Wu D, Li A and Ming N 2003 *Microelectron. Eng.* **66** 773

[5] Sugibuchi K, Kurogi Y and Endo N 1975 *J. Appl. Phys.* **46** 2877

[6] Debasis D, Tanmay G K and Panchanan P 2007 *Solid State Sci.* **9** 57

[7] Tellier J, Boullay P, Jennet D B and Mercurio D 2008 *Solid State Sci.* **10** 177

[8] Vural Ö, Şafak Y, Altındal Ş and Türüt A 2010 *Curr. Appl. Phys.* **10** 761

[9] Roul B, Bhat T N, Kumar M, Rajpalke M K, Sinha N, Kalghatgi A T and Krupanidhi S B 2011 *Solid State Commun.* **151** 1420

[10] Altuntaş H, Bengi A, Aydemir U, Asar T, Çetin S Ş, Kars Î, Altındal Ş and Özçelik S 2009 *Mater. Sci. Semicond. Proc.* **12** 224

[11] Pakma O, Serin N, Serin T and Altındal Ş 2008 *Semicond. Sci. Technol.* **23** 105014

[12] Tataroğlu A and Altındal Ş 2009 *J. Alloys Compd.* **479** 893.

[13] Chand S and Kumar J 1996 *Appl. Phys.* A: *Mater.* **63** 171

[14] Demirezen S and Altındal Ş 2010 *Curr. Appl. Phys.* **10** 1188

[15] Dökme İ and Altındal Ş 2006 *Semicond. Sci. Technol.* **21** 1053

[16] Tung R T 1992 *Phys. Rev.* B **45** 13509.

[17] Gümüş A, Türüt A and Yalçın N 2002 *J. Appl. Phys.* **91** 245

[18] Werner J H and Guttler H H 1991 *J. Appl. Phys.* **69** 1522

[19] Wang Y H, Zhang Y M, Zhang Y M, Song Q W and Jia R X 2011 *Chin. Phys.* B **20** 087305

[20] Ru G P, Yu R, Jiang Y L and Ruan G 2010 *Chin. Phys.* B **19** 097304

[21] Altuntaş H, Altındal Ş, Shtrikman H and Özçelik S 2009 *Microelectron. Reliab.* **49** 904

[22] Chand S and Kumar J 1996 *Semicond. Sci. Technol.* **11** 1203

[23] Gökçen M, Tunç T, Altındal Ş and Uslu İ 2012 *Mater. Sci. Eng.* B: *Adv.* **177** 416

[24] Gökçen M, Tunç T, Altındal Ş and Uslu İ 2012 *Curr. Appl. Phys.* **12** 525

[25] Gökçen M, Altındal Ş, Karaman M and Aydemir U 2011 *Physica* B **406** 4119

[26] Card H C and Rhoderick E H 1971 *J. Phys.* D: *Appl. Phys.* **4** 1589

[27] Schmitsdorf R F, Kampen T U and Mönch W 1995 *Surf. Sci.* **324** 349

[28] Chung G S, Kim K S and Yakuphanoğlu F 2010 *J. Alloys Compd.* **507** 508